

**Electronic Supplementary Information (ESI) for**

**Engineering nanoscale p-n junction via the synergetic dual-doping of p-type boron-doped graphene hybridized with n-type oxygen-doped carbon nitride for enhanced photocatalytic hydrogen evolution**

Lutfi Kurnianditia Putri,<sup>a</sup> Boon-Junn Ng,<sup>a</sup> Wee-Jun Ong,<sup>b</sup> Hing Wah Lee,<sup>c</sup> Wei Sea Chang,<sup>d</sup> and Siang-Piao Chai<sup>a,\*</sup>

*<sup>a</sup> Chemical Engineering Discipline, School of Engineering, Monash University, Jalan Lagoon Selatan, Bandar Sunway, 47500 Selangor, Malaysia*

*<sup>b</sup> Institute of Materials Research and Engineering (IMRE), Agency for Science, Technology and Research (A\*STAR), 2 Fusionopolis Way, Innovis, 138634, Singapore*

*<sup>c</sup> Nanoelectronics Lab, MIMOS Berhad, Technology Park Malaysia, Kuala Lumpur 57000, Malaysia*

*<sup>d</sup> Mechanical Engineering Discipline, School of Engineering, Monash University, Jalan Lagoon Selatan, Bandar Sunway, 47500 Selangor, Malaysia*

\* Corresponding author.

Tel: +603-5514 6234; Fax: +603-5514 6207

E-mail address: [chai.siang.piao@monash.edu](mailto:chai.siang.piao@monash.edu)

(1) Supplementary figures

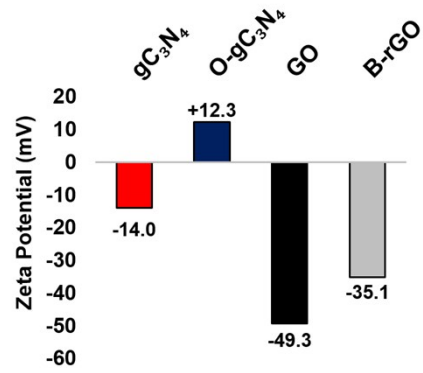


Fig S1 Zeta potential of gC<sub>3</sub>N<sub>4</sub>, O-gC<sub>3</sub>N<sub>4</sub>, GO and B-rGO.

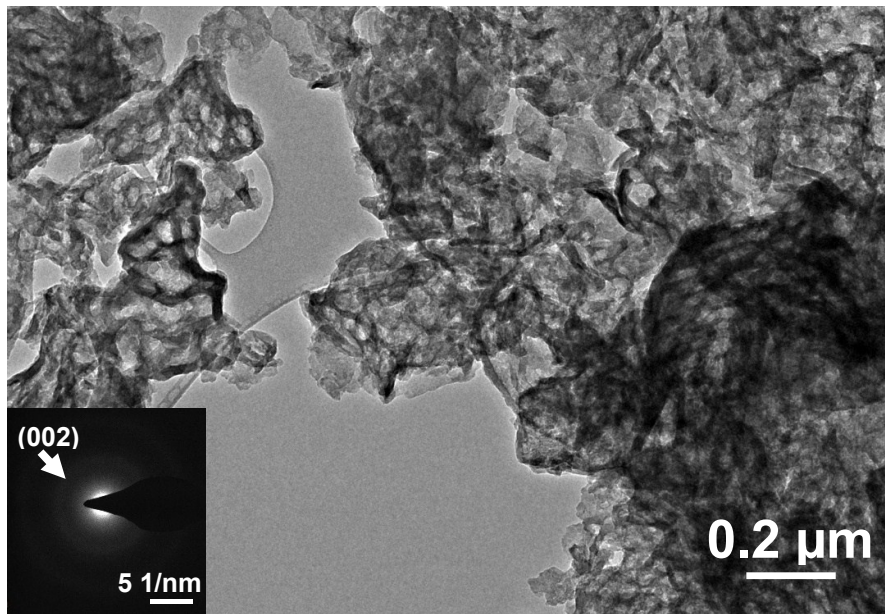
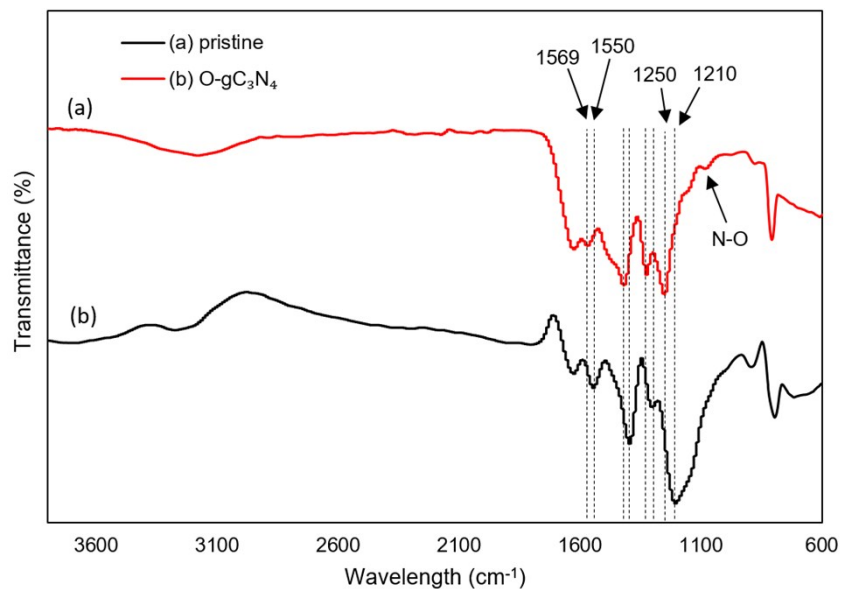
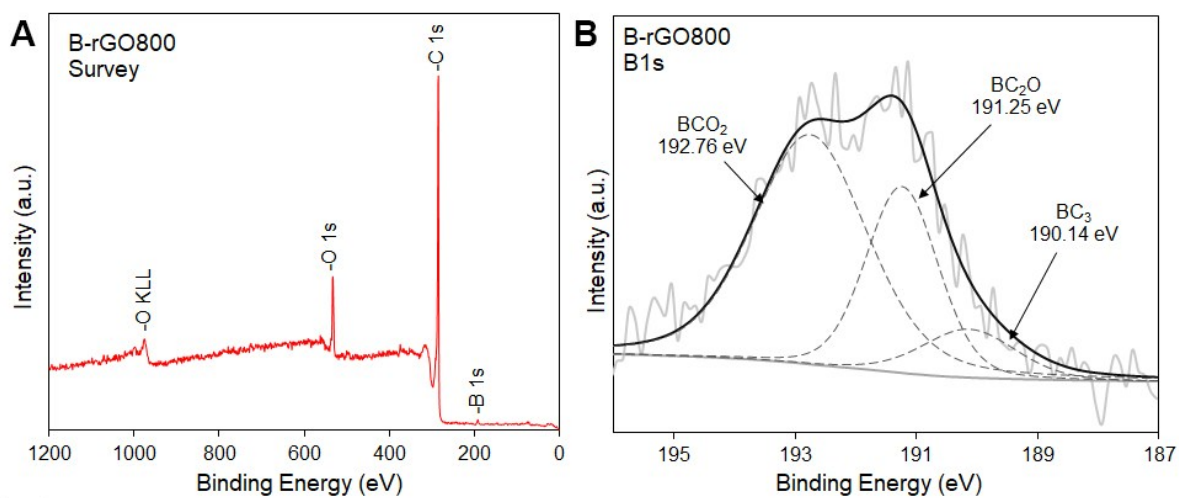


Fig. S2 TEM image SAED patterns (inset) of O-gC<sub>3</sub>N<sub>4</sub>.



**Fig. S3** FTIR images of  $g\text{-C}_3\text{N}_4$  and  $\text{O-gC}_3\text{N}_4$  samples.



**Fig. S4** XPS (a) Survey and (b) High resolution B 1s spectrum of B-rGO.

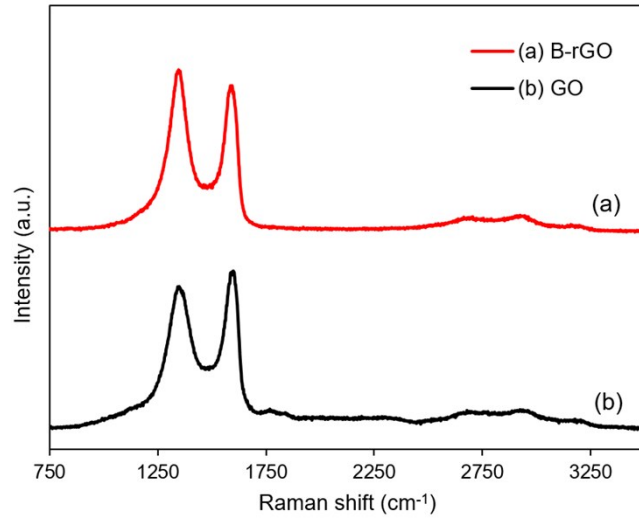


**Fig. S5** Raman spectra of GO and B-rGO samples.

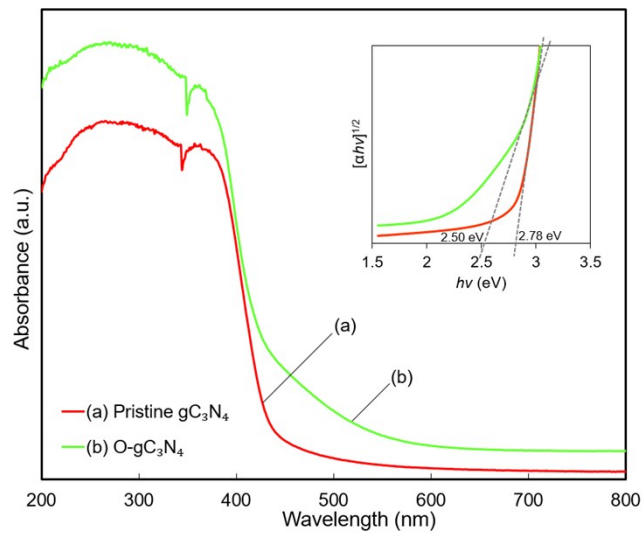


**Fig. S6** UV-Vis DRS of  $gC_3N_4$  and  $O-gC_3N_4$ . Inset figure shows the Kubelka-Munk plot for band gap determination.

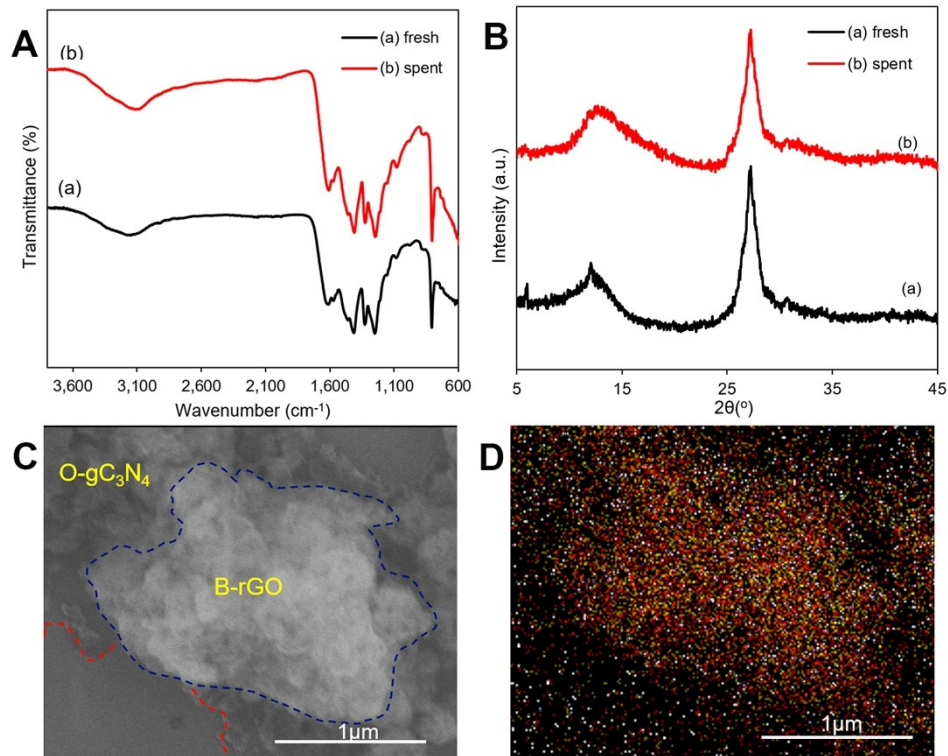


**Fig. S7** (A) XRD patterns, (B) FTIR spectra, (C) FESEM and (D) EDX elemental mapping comprising carbon (red), nitrogen (yellow) and oxygen (white) of used O-gC<sub>3</sub>N<sub>4</sub>/2B-rGO sample.

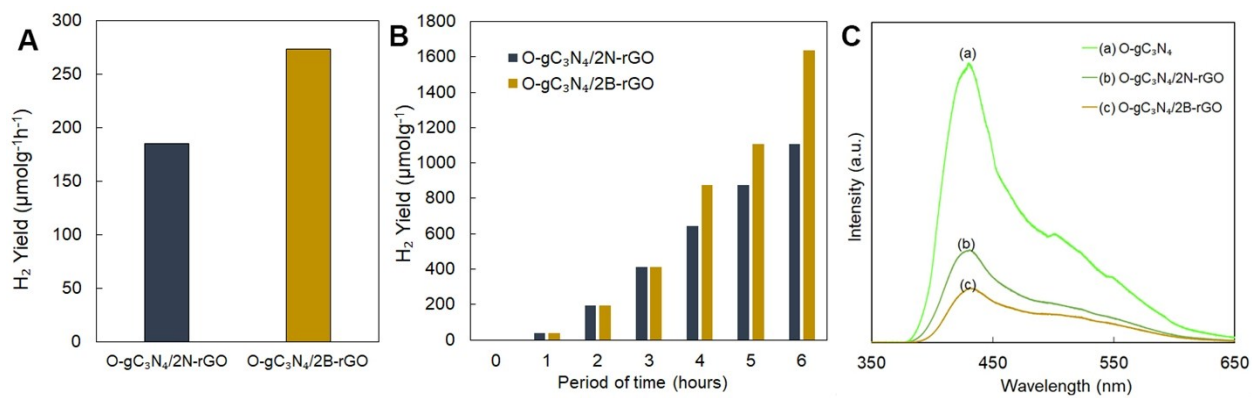


**Fig. S8** Photocatalytic hydrogen (a) total yield (b) temporal yield of O-gC<sub>3</sub>N<sub>4</sub>/N-rGO and O-gC<sub>3</sub>N<sub>4</sub>/B-rGO.

## (2) Apparent Quantum Yield (AQY) calculations

The AQY for H<sub>2</sub> evolution for the best sample O-gC<sub>3</sub>N<sub>4</sub>/2B-rGO was measured using the standard experimental setup. The final solution was irradiated by 500 W Xe lamp equipped with a 420 nm optical band-pass filter and subject to react for 6 h. The amount of H<sub>2</sub> evolved in the duration of 6 h was 125.24 μmolg<sup>-1</sup>. The average intensity of irradiation was determined to be 10 mW/cm<sup>2</sup> by an AvaSpec-ULS2048 spectrometer. The irradiation area was measured to be 14.13 cm<sup>2</sup>. Finally, the AQY was then estimated as follows:<sup>1</sup>

$$\begin{aligned} \text{QE} &= \frac{2 \times \text{the number of evolved } H_2 \text{ molecules}}{\text{the number of incident photons}} \times 100 \\ &= \frac{2 \times 6.02 \times 10^{23} \times 125.24 \times 10^{-6}}{10 \times 10^{-3} \times 14.13 \times 420 \times 6 \times 3600 \times 10^{-9}} \times 100 \\ &\quad / 6.626 \times 10^{-34} \times 3 \times 10^8 \\ &= 2.34\% \end{aligned}$$

### (3) Kelvin Probe Force Microscopy (KPFM) measurements

Kelvin Probe Force Microscopy (KPFM) was applied to indirectly measure changes in Fermi level. KPFM measures the contact potential difference between sample surface and AFM tip,  $V_{CPD}$ . When the tip  $\phi_{tip}$  work function is known, which can easily be found via calibration with gold leads ( $\phi_{tip} = \phi_{Au} + eV_{CPD}$ ), the work function of the sample is given by the equation  $\phi_s = \phi_{tip} - eV_{CPD}$ .<sup>2</sup> Work function is related to fermi level by the equation  $\phi = E_{vacuum} - E_{Fermi}$ . However, since the experiment is conducted under ambient conditions and due the high sensitivity nature of the instrument, slight alterations in the environment could significantly affect  $V_{CPD}$  readings. As no effort was taken to keep the recording conditions stable (under ultra-high vacuum condition), measuring the absolute value of  $\phi_s$  will not generate accurate results. However, these local variations of the work function can be expressed independent of  $\phi_{tip}$  by  $\Delta\phi_s = -e\Delta V_{CPD}$  with a common reference sample, in this case FTO. Although accurate absolute work function value of the samples could not be obtained, the relativity of their work function values could be retrieved.

Fig. S9(A) showed the topography (left) and corresponding  $V_{CPD}$  (right) of FTO and B-rGO in third dimension. FTO base had its characteristic blotchy feature and coated B-rGO on FTO resulted in the jump in the height profile. This step increase in height is translated in the potential map by a drop in  $V_{CPD}$ . This transition in height and potential occurred at the same position indicating the boundary of the two distinct materials. Fig. S9(B) showed the histogram analysis of the scanned area for 3 samples. Gaussian fitting reveals the average values of  $\Delta V_{CPD}$  are -190 mV, +750 mV and +350 mV for B-rGO, O-gC<sub>3</sub>N<sub>4</sub> and O-gC<sub>3</sub>N<sub>4</sub>/B-rGO respectively. This indicated Fermi levels of O-gC<sub>3</sub>N<sub>4</sub> and B-rGO equilibrate to a single in-between fermi level value, thus verifying the formation of a *p-n* junction.

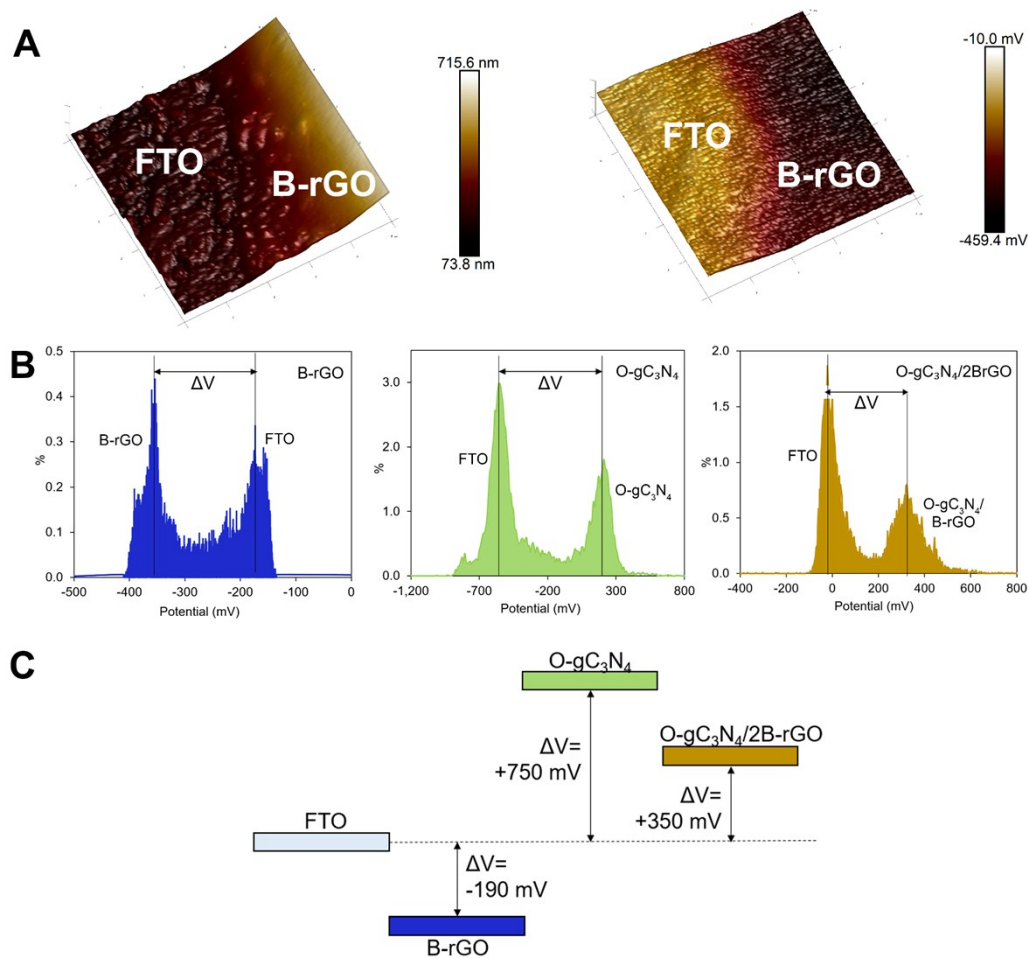


**Fig. S9** (A) 3D topography image (left) and Kelvin probe data i.e. surface potential map (right) at the FTO/B-rGO boundary. (B) Histogram analysis of the acquired Kelvin probe data. The two peaks are attributed to FTO and respective sample as indicated. (C) Schematic illustration of the work function position of samples relative to FTO.

## References

- [1] Y. Zhong, Y. Shao, F. Ma, Y. Wu, B. Huang and X. Hao, *Nano Energy*, 2017, **31**, 84-89.
- [2] A. Liscio, V. Palermo and P. Samorì, *Accounts Chem. Res.*, 2010, **43**, 541-550.